Journal of Alloys and Compounds 515 (2012) 26–31

Contents lists available at SciVerse ScienceDirect

Journal of Alloys and Compounds

journal homepage: www.elsevier.com/locate/jallcom

Structural phase transition, elastic and electronic properties of TmSb and YbSb: A LSDA + U study under pressure

Dinesh C. Gupta*, Sanjay K. Singh

Condensed Matter Theory Group, School of Studies in Physics, Jiwaji University, Gwalior 474 011, India

ARTICLE INFO

Article history:
Received 8 August 2011
Received in revised form
27 September 2011
Accepted 30 September 2011
Available online 8 October 2011

Keywords:
Rare-earth compounds
Phase transition
Electronic structure
Elastic properties
Debye temperature

ABSTRACT

The full-potential linear augmented plane wave plus local orbital method employing the local spin-density approximation (LSDA) along with Hubbard-U corrections and spin–orbit coupling has been used to study the electronic, structural, phase transition and elastic properties of TmSb and YbSb. Under compression they undergo first-order structural transition from B1 → B2 phase. The computed phase transition pressures are 21.74 and 13.57 GPa which agrees well with their measured values ~22.0 and 13 GPa. The structural properties *viz.*, equilibrium lattice constants, bulk modulus and its pressure derivative and volume collapse are also in closer agreement with their experimental data. The elastic constants and their combinations: Young's and Shear moduli, Poisson's ratio, Zener anisotropy factor, Lame's coefficients, Kleinman parameter and Debye temperature of these compounds have been computed at normal pressure. These values are in good agreement with experimental data. The LSDA + U strategy shows significant impact on the energy levels of the occupied and unoccupied 4f states in the electronic structure of both the compounds. The LSDA + U method provides better description of crystal properties of present system.

© 2011 Elsevier B.V. All rights reserved.

1. Introduction

The rare-earth (RE) monopnictides form an interesting family of materials and attracted the attention of researchers due to their unusual structural, electronic and elastic properties, despite their simple crystal structure [1–6]. They are, generally, semiconductors or semi-metals. Their electronic and magnetic properties are sensitive to temperature, pressure and impurity effects. The Tm and Yb ions in these compounds are predominantly trivalent with two and one 4f holes. The 4f bands are generally narrow and significantly different from the bands dominated by s, p and d states; there exists strong on-site Coulomb repulsion between the highly localized electrons [6 and references therein]. This makes the independent particle approximation no longer valid and calculation based on local spin density approximation (LSDA) fails to describe the role of RE 4f electrons correctly. Attempts beyond LSDA have the common idea to distinguish occupied and unoccupied 4f states. To explain the behavior of RE 4f electrons, many-body effects must be taken into account and calculations beyond LSDA are crucial. One possibility is to approximate the self-energy by introducing the Coulomb repulsion (Hubbard-U) as an additional parameter with spin–orbit coupling (SOC) to the one particle (LSDA) equations for a quasi-particle band structure.

Several experimental studies are reported in literature [1–3] on LnSb compounds. The high pressure structural properties of these compounds have been measured by powder X-ray diffraction (XRD) using synchrotron radiation up to 60 GPa at room temperature [1,2], which shows that TmSb and YbSb are stable in B1 phase and transform to B2 phase at ~22 and 13 GPa. Mullen et al. [3] have reported the magnetic, elastic, and thermal properties of the LnSb series, while Li et al. [4] have investigated the magnetic and thermal properties of the Ytterbium monopnictdes. The LnSb compounds have also been the subject of theoretical works: Temmerman et al. [5] and Svane et al. [6] have investigated the electronic configuration of Yb compounds by different *ab initio* methods, while Soni et al. [7] have computed the structural, elastic and thermal properties of antimonides of Ho, Er and Tm by a simple interionic potential. They have reported phase transition pressure (P_T) at 27, 33.2 and 29.8 GPa for these antimonides which are away from the measured data [1]. For the purpose of comparison, they have used the experimental values as 31, 35 and 31 GPa for these antimonides which are actually the data for high pressure transformed CsCl phase instead of P_T. As such, the structural, electronic and elastic properties of these compounds have not been studied systematically at ambient and high pressures by *ab initio* method. We aimed here to investigate theoretically the structural, electronic, phase transition and elastic properties of theoretically less explored TmSb and YbSb compounds. The lattice constant, bulk modulus (B_0), and its

* Tel.: +91 751 2442777; fax: +91 751 2442784.
E-mail addresses: sosfizix@gmail.com, sosfizix@yahoo.co.in (D.C. Gupta).

0925-8388/$ – see front matter © 2011 Elsevier B.V. All rights reserved.
doi:10.1016/j.jallcom.2011.09.098

pressure derivative (B_0'), second-order elastic constants (C_{ij}), Zener anisotropy factor (A), Poisson's ratio (σ), Young's (Y) and shear (G) moduli, shear and stiffness constant (C_S and C_L), Kleinman parameter (ξ), Lame's coefficients (μ, λ), elastic wave velocities ($\upsilon_l, \upsilon_t, \upsilon_m$), density ($\rho$) and Debye temperature (θ_D) are computed in two different B1 and B2 phases by LSDA + U with SOC method as implemented in WIEN2k [8]. The computed results are in good agreement with the available experimental [1–3] and better than earlier theoretical results [7]. The electronic band structures and total density of states (DOS) in B1 and B2 phases have also been computed. Such studies are important not only for these compounds but also valuable to understand mechanism of interaction in other lanthanieds series. We have briefly discussed the methodology of computations in next section followed by discussions on the results obtained for the structural phase transition, electronic structure as well as mechanical and other thermophysical properties of these compounds in Section 3. Finally, the paper contents have been concluded in last Section 4.

2. Methodology of computations

The calculations were performed using the full-potential linear augmented plane wave (FP-LAPW) method. The application of plain LSDA calculations to f-electron systems is often inappropriate because of the correlated nature of the shell. We have adopted LSDA + U with SOC approach [9] to better account for the onsite f-electron correlations. In this method, an orbitally dependent potential is introduced for the chosen set of electron states, which is present in 4f states of lanthanides. This additional potential has an atomic Hartree–Fock form but with screened Coulomb and exchange interaction parameters. The optimized value of Coulomb screening potential (U) and the exchange coupling (J) for the RE 4f orbitals (for Thulium $U = 8.84$ and $J = 0.1$ eV, and Ytterbium $U = 10.2$ and $J = 0.1$ eV) have been calculated in the super-cell approximation using the method of Madsen and Novak [10]. The SOC has been included on the basis of the second variation method by using scalar relativistic wave function [8]. In this method, the wave function, charge density and potential are expanded by spherical harmonic function inside nonoverlapping spheres surrounding the atomic sites (muffin-tin (MT) spheres) and by a plane-wave (PW) basis set in the remaining space of the unit cell (interstitial region). Tm: $6s^2\ 5p^6\ 5d^1\ 4f^{12}$, Yb: $6s^2\ 5p^6\ 5d^1\ 4f^{13}$ and Sb: $4d^{10}\ 5s^2\ 5p^3$ states are treated as valance electrons. The convergence parameter $R_{MT}K_{max}$, which controls the size of basis set in the calculations, was set to 8. The R_{MT} radii were taken as 2.95, 3.1 and 2.3 Å for Tm, Yb and Sb, respectively. The valance wave functions inside MT spheres were expanded up to $l_{max} = 10$, while the charge density was Fourier expanded up to $G_{max} = 23$ Å^{-1}. The self-consistent calculations are converged up to an accuracy of 10^{-5} Ry in the total energy of the system. The integrals over the Brillouin zone (BZ) are performed in mesh of $9 \times 9 \times 9$ for both B1 and B2 phases in the irreducible BZ using the Monkhost-Pack special k-points approach [11]. Both the PW cut-off and the number of k-points were varied and optimized to ensure total energy convergence.

Table 1
The values of lattice parameter (a in Å), bulk modulus (B_0 in GPa) and its pressure derivative (B_0') for LnSb in B1 and B2 phases.

Solids	Phase	A	B_0	B_0'	References
TmSb	NaCl	6.055	57.41	4.29	Present
		6.084	–	–	Expt. [1]
		–	70.04	5.86	Others [7]
	CsCl	4.61	59.00	3.97	Present
YbSb	NaCl	6.074	59.30	4.77	Present
		6.081	52 ± 2	7.5 ± 0.8	Expt. [2]
	CsCl	4.65	56.40	3.78	Present

6.055 and 6.074 Å for TmSb and YbSb, respectively which are very close to the experimental values ($a = 6.084$ and 6.082 Å).

3. Results and discussions

3.1. Structural and phase transition properties

The NaCl (B1 phase) to CsCl (B2 phase) structural transition and related properties of TmSb and YbSb have been analyzed by computing the total energy of the primitive unit cell as a function of volume fitted to Murnaghan's equation of state [12]. The variation of total energy with cell volume for B1 and B2 phases have been shown in Fig. 1(a and b). It is clear from these figures that phase transition occurs as the curves of B1 and B2 phases intersect each other. The total energy is lowest in B1 phase as compared to that in B2 phase and hence B1 phase stabilizes at ambient conditions. The equilibrium cell volume in the B1 phase at ambient pressure is estimated to be 55.52 and 56.02 Å^3 with lattice parameter (a) as 6.055 and 6.074 Å for TmSb and YbSb, respectively which are very close to the experimental values ($a = 6.084$ and 6.081 Å) [1,2] and deviate marginally by 0.477% and 0.132% from their measured values. The ground state properties of these compounds have been calculated from the total energy of B1 and B2 phases at different volumes around the equilibrium cell volume (V_0). The plots of total energies *vs.* cell volume in these structures are drawn in Fig. 1(a and b) for TmSb and YbSb. To determine the ground state properties, we have calculated the equilibrium lattice constant (a), bulk modulus (B_0) and its pressure derivative (B_0'). The calculated structural parameters of these compounds in both the phases have been summarized in Table 1 together with the available experimental

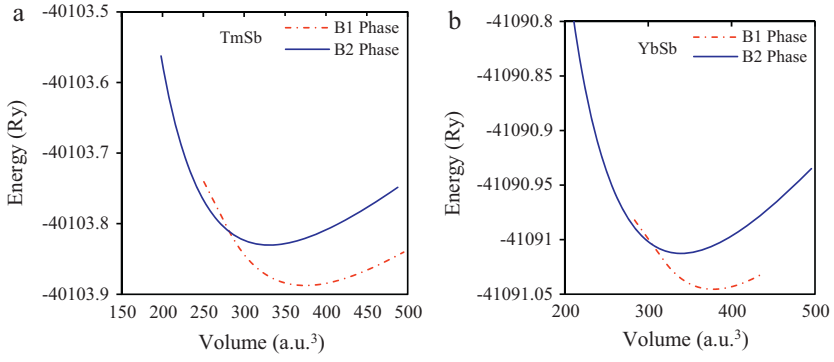

Fig. 1. Total energy *vs.* cell volume in B1 and B2 phases of (a) TmSb; (b) YbSb.

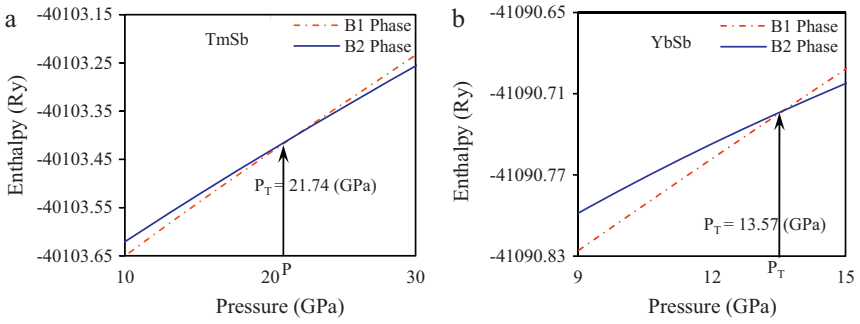

Fig. 2. Pressure variation of enthalpy for (a) TmSb; (b) YbSb.

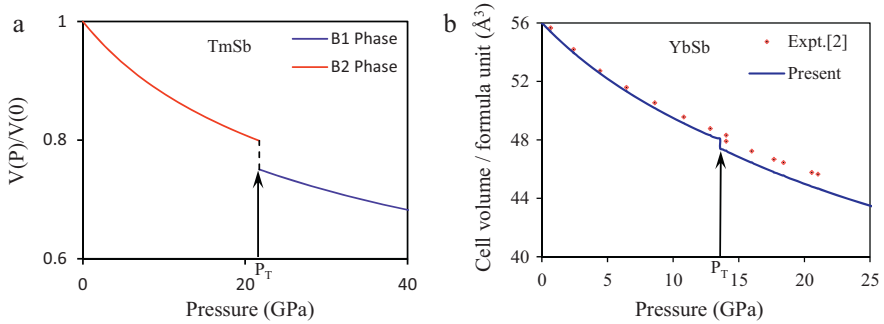

Fig. 3. Equation of states for (a) TmSb; (b) YbSb.

[1,2] and other theoretical [7] values. It may be seen from this table that our computed values for a, B_0 and B_0' are closer to measured data and better than those obtained by earlier theoretical workers [7] from model potential. The calculated bulk modulus of YbSb is comparatively more as compared to TmSb. It suggests that TmSb is comparably more compressible than YbSb. With the application of high pressures, the calculations show that a new crystal phase appears in these compounds and the relative stability of two crystal structures requires more precise calculations. To discuss the relative stability of the two phases, we have estimated the free enthalpy ($H = E + PV$; where E = total energy of the system, P = pressure and V = unit cell volume) for the concerned phases at different pressures. The enthalpy *vs.* pressure graphs for TmSb and YbSb in B1 and B2 phases have been displayed in Fig. 2(a and b). It may be seen from these figures that the enthalpy remains minimum up to 21.73 GPa in parent (B1) phase for TmSb and 13.56 GPa for YbSb. At 21.74 and 13.57 GPa, enthalpies in both the phases become equal showing that both the phases are in equilibrium at this pressure, hence structural phase transformation occurs at this point, which is marked by arrow as P_T in these figures. On further increasing the pressure beyond P_T, enthalpy is lowered in B2 phase as compared to that in B1 phase *i.e.*, B2 phase stabilizes with more minimum enthalpy in these compounds beyond P_T.

The variation of reduced volume ($V(P)/V(0)$) with pressure have been plotted in Fig. 3(a and b) to obtain the equation of state (EOS) of these materials and to understand the mechanism of transformation. It is clear from Fig. 3(a) that the volume of TmSb decreases smoothly up to P_T. At P_T, an abrupt decline in volume is observed, which is associated with first-order phase transformation showing structural change from B1 → B2 phase. From Fig. 3(b) similar trend of variation has been observed in YbSb except that it occurs with different magnitudes of volume collapse at P_T. The values of % discontinuity in reduced volume at P_T ($\Delta V(P_T)/V(0)$) along with P_T have been reported in Table 2 along with experimental data. It is seen that our values are quite close to the measured value for YbSb [2], hence LSDA + U method is capable to predict correctly the stable and high pressure crystallographic structures as B1 and B2 phases in TmSb and YbSb.

3.2. Electronic properties of TmSb and YbSb

The LSDA + U scheme with SOC has been used to compute the electronic structure in B1 phase at the equilibrium lattice constant and in B2 phase just after P_T. The electronic structure and total density of state (DOS) for TmSb with $U = 8.84$ eV and $J = 0.1$ eV has been plotted in Fig. 4. The conduction band is mainly due to 5d and 6p states of Tm, along with empty states 4f of Tm. It is clear from this figure that the lowest band around −10.57 to −7.83 eV is mainly due to the Sb s character which hybridized with occupied Tm 4f states (may be seen as sharp peak in the total density of state) while two empty unoccupied 4f energy levels are located around 1 eV above the Fermi energy (E_F) and hybridized with Tm 5d states and 4p states of Sb. The six Sb p bands positioned at around −4.75 to 0.84 eV are separated from the s bands by an energy gap of ∼3.1 eV. It is clear from Fig. 4 that two bands from conduction band dip down the Fermi level making them semi-metallic. Besides this, we have computed the band structure and the total density

Table 2
The values of the phase transition pressure (P_T in GPa), the % volume collapse at P_T ($\Delta V(P_T)/V(0)$) for LnSb.

Solids	P_T	$\Delta V(P_T)/V(0)$	References
TmSb	21.74	4.8	Present
	22	–	Expt. [1]
	29.80	5.70	Others [7]
YbSb	13.57	1.14	Present
	13.00	1.00	Expt. [2]

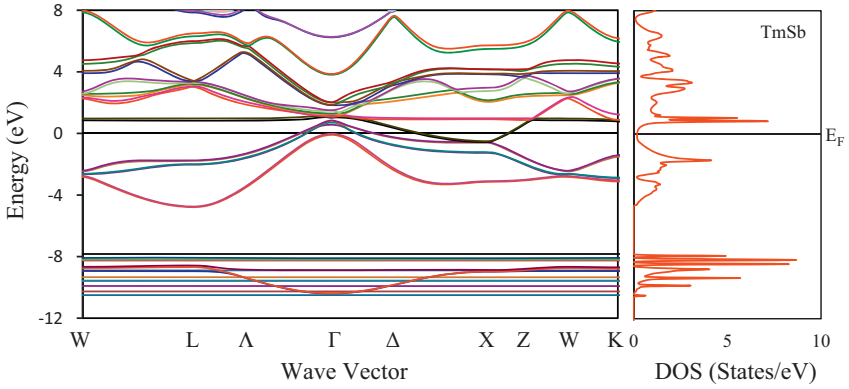

Fig. 4. Band structure and DOS of TmSb with LSDA + U and spin–orbit coupling in B1 phase at ambient conditions.

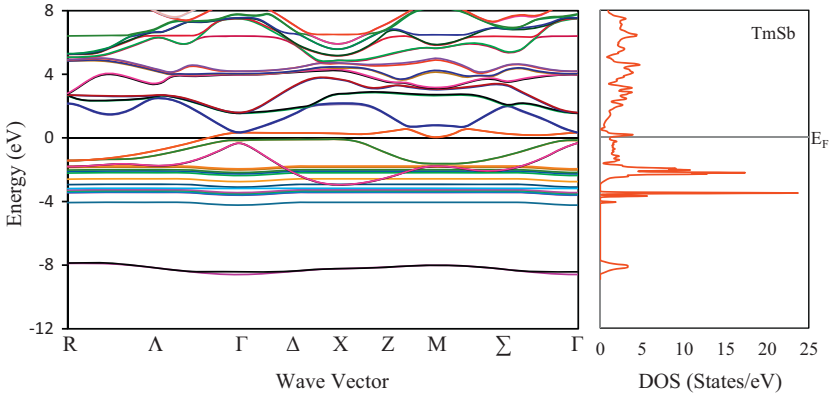

Fig. 5. Band structure and DOS of TmSb with LSDA + U and spin–orbit coupling in B2 phase just after the P_T.

of state of TmSb in B2 phase also and plotted them in Fig. 5. It is seen that the width of 5p states of Sb get narrowed under pressure and they hybridize with f-bands. Under compression, the f-bands shift upward and found around −1.79 to −4.07 eV as seen in the corresponding peaks in DOS. Two of the p-bands cross the Fermi level and touch the bottom of the conduction band showing metallization. The electronic band structure and total density of states of YbSb with $U = 10.2$ eV and $J = 0.1$ eV along the high-symmetry directions in the BZ of B1 phase have been depicted in Fig. 6. Similar trend of electronic structure is observed as found in TmSb except the difference in the position of the bands. YbSb has thirteen occupied Yb 4f states and one empty state. YbSb is also semi-metallic. The high pressure electronic structure in B2 phase just after P_T has also been computed with corresponding DOS and plotted in Fig. 7 for YbSb. It is found that it also follow the same trend as found in TmSb.

3.3. Elastic properties

The elastic moduli have been calculated from the variation of the total energy under volume-conserving strains. Elastic properties of a solid are especially important for mechanical applications. The values of elastic constants provide a link between

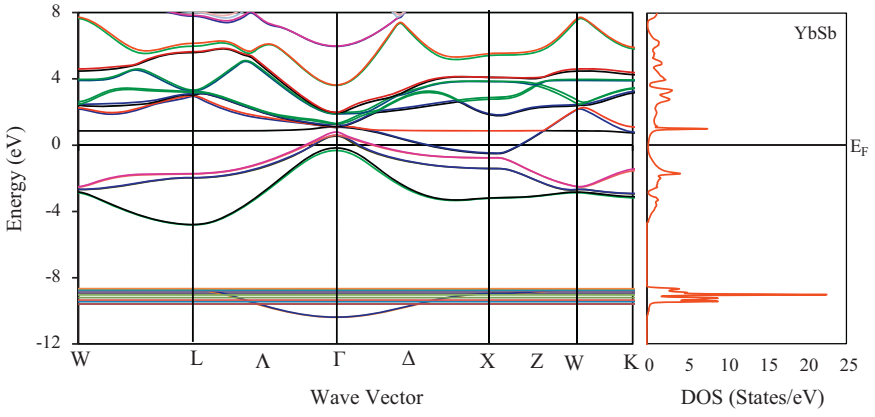

Fig. 6. Band structure and DOS of YbSb with LSDA + U and spin–orbit coupling in B1 phase at ambient conditions.

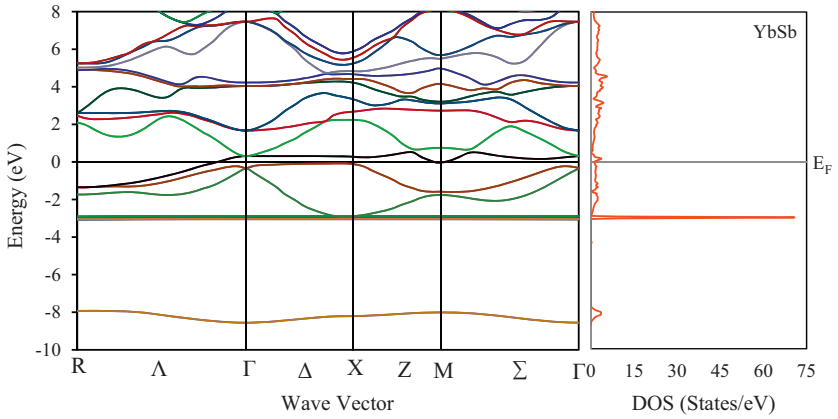

Fig. 7. Band structure and DOS of YbSb for LSDA + U with spin–orbit coupling and in B2 phase just after the P_T.

the mechanical and dynamical behaviors of the crystals. Elastic properties are also thermodynamically related to the specific heat, thermal expansion, melting point and Grüneisen parameter, etc. We have calculated the second-order elastic constants (SOECs) of these compounds in B1 phase at ambient conditions by using the method developed by Mehl [13]. In present calculations, small lattice distortion has chosen in order to remain within elastic domain of the crystal. A cubic structure is characterized by three independent elastic constants namely C_{11}, C_{12}, and C_{44}. The computed values of elastic constants C_{ij} for TmSb and YbSb compounds in B1 phase are presented in Table 3 along with experimental data. These values agree well with the measured data [3] and better than those reported by other theoretical worker [7]. Furthermore, all the elastic constants satisfy the required stability criterion [14]: $(C_{11} - C_{12}) > 0$, $(C_{11} + 2C_{12}) > 0$, $C_{11} > 0$, $C_{44} > 0$ hence, these compounds are stable in B1 phase against elastic deformation. Besides this, we have also computed various combinations of these SOECs *viz.*, Y, G, C_S, C_L, ξ, σ, A, μ, λ and Cauchy pressure at ambient conditions.

Table 3
The values of elastic properties (in GPa), and σ, A and ξ (dimensionless) for LnSb in B1 phase.

Parameters	TmSb	YbSb	References
C_{44}	20.74	12.51	Present
	26.80	–	Expt. [3]
	24.70	–	Others [7]
$C_{12} - C_{44}$	−12.34	−3.12	Present
G	41.94	37.52	Present
	43.08	–	Expt. [3]
	42.10	–	Others [7]
Y	101.24	92.98	Present
	154.30	–	Others [7]
σ	0.21	0.24	Present
	0.13	–	Others [7]
A	0.28	0.17	Present
	0.40	–	Expt. [3]
	0.36	–	Others [7]
C_S	73.75	75.04	Present
	67.50	–	Expt. [3]
C_L	102.89	96.93	Present
ξ	0.20	0.21	Present
μ	41.94	37.52	Present
λ	29.61	34.40	Present

$$C_S = \frac{C_{11} - C_{12}}{2}, \quad C_L = \frac{C_{11} + C_{12} + 2C_{44}}{2},$$

$$G = \frac{C_{11} - C_{12} + 3C_{44}}{5}, \quad Y = \frac{9B_0G}{3B_0 + G}, \quad A = \frac{2C_{44}}{C_{11} - C_{12}},$$

$$\xi = \frac{C_{11} + 8C_{12}}{7C_{11} + 2C_{12}}, \quad \sigma = \frac{3B_0 - Y}{6B_0}, \quad \mu = \frac{Y}{2 + 2\sigma},$$

$$\lambda = \frac{\sigma Y}{(1+\sigma)(1-2\sigma)}, \quad C_{12} - C_{44} = 2P$$

The calculated values of A are 0.28 and 0.17 for TmSb and YbSb while experimental value is 0.4 for TmSb [3]. It is clear that A is well below unity for these compounds and hence these compounds are anisotropic (as "A" approaches unity the crystal becomes isotropic). Our results show negative values of Cauchy pressure in these compounds which is a consequence of the hybridization of the unstable 'f' band. This hybridization may be responsible for the decrease in Ln–Ln distance and therefore for small value of elastic constant C_{12}. Pettifor [15] suggested that the angular character of atomic bonding in metals and compounds, which is also related to the ductile nature, could be described by Cauchy pressure. For metallic bonding, it must be typically positive and negative for directional bonding with angular character. The larger negative pressure represents more directional character. The calculated Cauchy pressure is −12.34 and −3.12 GPa in these compounds which confirms that both TmSb and YbSb are partial covalent (directional) in nature.

A simple relationship to explain the plastic nature of the materials in terms of elasticity has been proposed by Pugh [16]. The shear modulus represents the resistance to plastic deformation, while the bulk modulus represents the resistance to fracture. A high B_0/G ratio is associated with ductile nature, whereas a low value corresponds to brittle nature of the material. The critical value which separates ductile and brittle materials is around ∼1.75. If $B_0/G > 1.75$ the material behaves in a ductile manner otherwise it is brittle. Our calculated value of B_0/G is 1.36 and 1.58 for TmSb and YbSb which are less than the critical value and hence both the materials are brittle by nature. On the other hand, Frantsevich et al. [17] have also explained the ductile/brittle nature of the materials on the basis of the Poisson's ratio. Accordingly, the material to be brittle in nature, σ must be ≤0.33, else the material is ductile. The calculated values of σ are less than the critical value hence it also classifies both the materials as brittle under ambient conditions. Hence, our results satisfy both the conditions for these materials to be brittle.

Table 4
The values of density (ρ in gm/cm^3), the longitudinal, transverse and average sound velocity (υ_l, υ_t and υ_m in m/s) and Debye temperature (θ_D in K) for LnSb in B1 phase.

Solids	ρ	υ_l	υ_t	υ_m	θ_D	References
	8.7	3645.5	2216.2	2448.5	241.0	Present
TmSb	8.6	–	–	–	237.0	Expt. [3]
	8.6	3837.0	2215.3	2459.0	237.0	Others [7]
YbSb	8.8	3580.0	2096.0	2324.1	228.0	Present

3.4. Debye temperature

Debye temperature is an important fundamental parameter closely related to elastic constants, specific heat and melting temperature. We have used the classical relation to compute θ_D

$$\theta_D = \frac{h}{k_B}\left[\frac{3n}{4\pi V_a}\right]^{1/3}\upsilon_m$$

Here, n is the number of atoms per formula unit, V_a is atomic volume while average speed of sound (υ_m) in the polycrystalline materials is $\upsilon_m = [1/3((2/\upsilon_t^3) + (1/\upsilon_l^3))]^{-1/3}$ with υ_l and υ_t as the longitudinal and transverse sound velocities which can be obtained using the method discussed elsewhere [18]

$$\upsilon_l = \sqrt{\frac{\left[C_{11} + \frac{2}{5}(2C_{44} + C_{12} - C_{11})\right]}{\rho}},$$

$$\upsilon_t = \sqrt{\frac{\left[C_{44} + \frac{1}{5}(2C_{44} + C_{12} - C_{11})\right]}{\rho}}$$

Here, ρ is the mass density per unit volume. The calculated values of sound velocities, θ_D as well as ρ of TmSb and YbSb have been reported in Table 4 along with experimental data. It is observed that θ_D decreases with increasing atomic number of RE atom, Tm to Yb and these are close to the measured values [3]. Slight variation in these values, from experimental data, is due to the fact that we have computed these values at equilibrium conditions while the experimental data is at 200 K.

4. Conclusions

This paper deals with the computations of electronic, structural, phase transition and elastic properties of TmSb and YbSb, using the FP-LAPW + lo method employing LSDA + U with SOC approach. The computed values of a, B_0, B_0', P_T, EOS, $\Delta V(P_T)/V(0)$, SOECs and their combinations, υ_m, υ_l, υ_t, ρ, θ_D, etc. are explained well and show good agreement with experimental data. These materials show first-order phase transition from six-fold coordinated B1 phase to eight-fold coordinated B2 phase under compression. The electronic structure has been computed in both B1 and B2 phases to analyze the effect of pressure on the nature of bands in these strongly correlated compounds. The LSDA + U with SOC method predicted semi-metallic nature of these compounds at ambient conditions and metallization at high pressures. Some of the results, estimated probably for first time, will be tested by future workers.

Acknowledgment

The work is supported by the Department of Science and Technology (DST), New Delhi, India.

References

[1] I. Shirotani, J. Hayashi, K. Yamanashi, N. Ishimatsu, O. Shimomura, T. Kikegawa, Phys. Rev. B 64 (2001) 132101–132104.
[2] J. Hayashi, I. Shirotani, T. Adachi, O. Shimomura, T. Kikegawa, Philos. Mag. 84 (2004) 3663–3670.
[3] M.E. Mullen, B. Lüthi, P.S. Wang, E. Bucher, L.D. Longinotti, J.P. Maita, H.R. Ott, Phys. Rev. B 10 (1974) 186–199.
[4] D.X. Li, A. Oyamada, K. Hashi, Y. Haga, T. Matsumura, H. Shida, T. Suzuki, T. Kasuya, A. Dönni, F. Hulliger, J. Magn. Magn. Mater. 140 (1995) 1169–1170.
[5] W.M. Temmerman, Z. Szotek, A. Svane, P. Strange, H. Winter, A. Delin, B. Johansson, O. Eriksson, L. Fast, J.M. Wills, Phys. Rev. Lett. 83 (1999) 3900–3903.
[6] A. Svane, W.M. Temmerman, Z. Szotek, L. Petit, P. Strange, H. Winter, Phys. Rev. B 62 (2000) 13394–13399.
[7] P. Soni, G. Pagare, S.P. Sanyal, J. Phys. Chem. Sol. 71 (2010) 1491–1498.
[8] P. Blaha, K. Schwarz, G.K.H. Madsen, D. Kvasnicka, J. Luitz, in: K. Schwarz (Ed.), WIEN2k, An Augmented Plane Wave + Local Orbitals Program for Calculating Crystal Properties, Technische Universitat, Wien, Austria, 2001, ISBN 3-9501031-1-2.
[9] V.I. Anisimov, I.V. Solovyev, M.A. Korotin, M.T. Czyzyk, G.A. Sawatzky, Phys. Rev. B 48 (1993) 16929–16934.
[10] G.K.H. Madsen, P. Novak, Europhys. Lett. 69 (2005) 777–783.
[11] H.J. Monkhost, J.D. Pack, Phys. Rev. B 13 (1975) 5188–5192.
[12] F.D. Murnaghan, PNAS 30 (1944) 244–247.
[13] M.J. Mehl, Phys. Rev. B 47 (1993) 2493–2500.
[14] D.C. Wallace, Thermodynamics of Crystals, John Wiley & Sons, New York, 1972, pp. 1–56.
[15] D.G. Pettifor, Mater. Sci. Technol. 8 (1992) 345–349.
[16] S.F. Pugh, Philos. Mag. 45 (1954) 823–843.
[17] I.N. Frantsevich, F.F. Voronov, S.A. Bokuta (Eds.), Elastic Constants and Elastic Moduli of Metals and Insulators, Naukova Dumka, Kiev, 1983, pp. 60–180.
[18] D.C. Gupta, S. Kulshrestha, J. Alloys Compd. 509 (2011) 4653–4659.